Weak imposition of boundary conditions for the gauge formulation of the incompressible Navier–Stokes equations

Kenny Wiratama[1] Stephen Roberts[2] Kenneth Duru[3]

(Received 30 December 2020; revised 5 October 2021)

Abstract

The projection method was first introduced by Chorin [*Bull. AMS* 73 (1967), pp. 928–931] and Temam [*Arch. Rat. Mech. Anal.* 33 (1969), pp. 377–385] as a computationally efficient numerical method to solve the incompressible Navier–Stokes equations. Despite its success in decoupling the computations of velocity and pressure, it suffers from inaccurate numerical boundary layers. As an effort to resolve this inaccuracy, E and Liu [*Int. J. Numer. Meth. Fluids* 34 (2000), pp. 701–710] proposed the gauge method, which is a reformulation of the Navier–Stokes equations in terms of an auxiliary vector field and a gauge variable. This method utilizes the freedom of choosing a boundary condition for the gauge variable to reduce the numerical coupling

DOI:10.21914/anziamj.v62.16117, Published 2022-02-07, as part of the Proceedings of the 19th Biennial Computational Techniques and Applications Conference. ISSN 1445-8810. (Print two pages per sheet of paper.)

between the considered variables. Nevertheless, the computational implementation of the boundary conditions for the auxiliary vector field is difficult in the context of finite elements since they involve either the normal or tangential derivative of the gauge variable. In order to circumvent this issue, we propose a weak formulation of the boundary conditions based on the symmetric Nitsche method. Computational results are presented to illustrate the accuracy of the proposed method.

Contents

1 Introduction

In this article, we consider the non-dimensionalized incompressible Navier–Stokes equations

$$\partial_t \mathbf{u} + (\mathbf{u} \cdot \nabla)\mathbf{u} = -\nabla p + \frac{1}{\mathrm{Re}} \Delta \mathbf{u} + \mathbf{f} \qquad \text{in } \Omega, \tag{1a}$$

$$\nabla \cdot \mathbf{u} = 0 \qquad \text{in } \Omega, \tag{1b}$$

where $\Omega \subset \mathbb{R}^2$ is a bounded domain with sufficiently smooth boundary Γ, $\mathbf{u}$ is the velocity, p is the pressure, and Re is the Reynolds number. We also

prescribe the above problem with the no-slip boundary condition

$$\mathbf{u} = \mathbf{0} \quad \text{on } \Gamma \tag{2}$$

and the initial condition

$$\mathbf{u}|_{t=0} = \mathbf{u}_0 \quad \text{in } \Omega. \tag{3}$$

Designing an efficient and accurate numerical scheme for problem (1)–(2) is a challenging task. In particular, one of the difficulties is the numerical implementation of the divergence-free condition (1b). A common approach is to treat this condition as a constraint, and then the method of Lagrange multipliers is utilized. This results in a saddle-point problem, which is computationally expensive for high-resolution numerical simulations [1].

The projection method was invented by Chorin [3] and independently by Temam [16] to efficiently compute numerical solutions of the incompressible Navier–Stokes equations. By omitting the pressure term in the momentum equation (1a), the method first computes an intermediate velocity field that does not necessarily satisfy the divergence-free condition. Then, by solving a Poisson problem, the intermediate velocity field is projected onto a space of a divergence-free vector field. Since the computations of velocity and pressure are decoupled, this approach avoids the need to a solve saddle-point system. However, this significant improvement in computational efficiency does come at a price. Specifically, the projection method produces inaccurate numerical boundary layers for the pressure [5].

E and Liu [6] introduced the gauge method as an effort to improve the projection method. As illustrated in Figure 1, utilizing the projection method to solve problem (1)–(2) with the same numerical setup described in Section 5 gives inaccurate numerical boundary layers, and hence the gauge method is proposed as a solution to this accuracy issue [18]. Furthermore, the computational efficiency of the projection method is well retained by the gauge method since the gauge method is able to computationally decouple the problem. This efficiency is mainly due to the gauge method reformulating

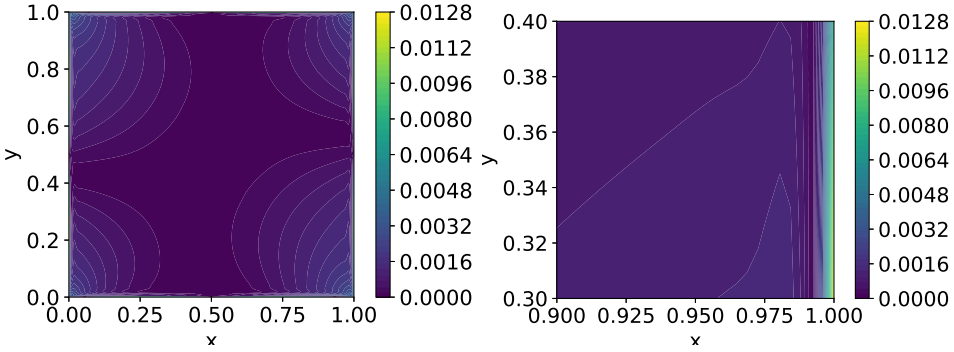

(a) Whole domain (b) Zoomed-in

Figure 1: Pressure error heatmaps obtained using the projection method.

the incompressible Navier–Stokes equations in terms of an auxiliary vector field and a gauge variable [17].

Some studies have been conducted to illustrate the accuracy of the gauge method [17, 4, 6, 2, 19], where finite difference methods were mainly used for spatial discretizations. The use of finite elements for spatial discretizations in gauge methods receives limited attention, and the numerical implementation of the boundary conditions for the auxiliary vector field is still a concern [4, 13]. In particular, these boundary conditions are complicated to implement using finite elements due to the presence of either a normal or tangential derivative of the gauge variable. One way to address this problem is by utilizing the gauge-Uzawa method, which was developed by Nochetto and Pyo [13, 14]. In this article, instead of using the gauge-Uzawa method, we resolve the implementation problem by imposing the boundary conditions in a weak sense using the symmetric Nitsche method [12]. Although this approach gives a complicated weak problem, the actual implementation is straightforward through the help of popular finite element packages such as FEniCS [10].

2 Gauge formulation

In this section, we briefly present the gauge formulation of the Navier–Stokes equations (1), which was proposed by E and Liu [4]. To begin with, we introduce a gauge variable ϕ, and then we define the auxiliary vector field as

$$\mathbf{m} = \mathbf{u} - \nabla\phi\,. \tag{4}$$

Substituting the above equation into equation (1a) gives

$$\partial_t\mathbf{m} + (\mathbf{u}\cdot\nabla)\mathbf{u} = \frac{1}{\mathrm{Re}}\Delta\mathbf{m} - \nabla\left(p + \partial_t\phi - \frac{1}{\mathrm{Re}}\Delta\phi\right) + \mathbf{f}\,. \tag{5}$$

Hence, we enforce the condition

$$p = \frac{1}{\mathrm{Re}}\Delta\phi - \partial_t\phi\,, \tag{6}$$

and equation (5) becomes

$$\partial_t\mathbf{m} + (\mathbf{u}\cdot\nabla)\mathbf{u} = \frac{1}{\mathrm{Re}}\Delta\mathbf{m} + \mathbf{f}\,. \tag{7}$$

The above equation specifies a time-dependent equation for the auxiliary vector field $\mathbf{m}$ without the pressure term p.

To obtain an equation for ϕ, we take the divergence of both sides of (4):

$$-\Delta\phi = \nabla\cdot\mathbf{m}\,, \tag{8}$$

where we have used the divergence-free condition (1b). Since the gauge variable ϕ has no physical meaning, we have the freedom to choose an unambiguous boundary condition for the Poisson problem (8). For instance, the homogeneous Neumann or Dirichlet boundary condition. In this article, we focus our attention on the homogeneous Neumann boundary condition

$$\partial_n\phi = 0 \quad \text{on } \Gamma, \tag{9}$$

where $\mathbf{n}$ is the normal vector to the boundary. This boundary condition and equation (2) imply that

$$\mathbf{m} \cdot \mathbf{n} = 0 \quad \text{and} \quad \mathbf{m} \cdot \boldsymbol{\tau} = -\partial_{\tau}\phi \quad \text{on } \Gamma, \tag{10}$$

which are the boundary conditions for equation (7). Here, $\boldsymbol{\tau}$ is the tangential vector to the boundary.

Remark 1. Using a similar argument, prescribing the homogeneous Dirichlet boundary condition $\phi = 0$ on Γ leads to corresponding boundary conditions for equation (5). In this case, the boundary conditions involve the normal derivative $\partial_{n}\phi$.

Remark 2. The numerical implementation of the boundary conditions (10) involves the computation of the tangential derivative $\partial_{\tau}\phi$. The non-variational nature of this term leads to implementation difficulties, especially when handling complex geometries [13].

In summary, the gauge formulation of the Navier–Stokes problem gives the following time-dependent problem for the auxiliary vector field:

$$\partial_{t}\mathbf{m} + (\mathbf{u} \cdot \nabla)\mathbf{u} = \frac{1}{\mathrm{Re}}\Delta\mathbf{m} + \mathbf{f}, \tag{11a}$$

$$\mathbf{m} \cdot \mathbf{n} = 0 \text{ and } \mathbf{m} \cdot \boldsymbol{\tau} = -\partial_{\tau}\phi \quad \text{on } \Gamma. \tag{11b}$$

Furthermore, the gauge variable is governed by

$$-\Delta\phi = \nabla \cdot \mathbf{m}, \tag{12a}$$

$$\partial_{n}\phi = 0 \quad \text{on } \Gamma. \tag{12b}$$

We observe from this reformulation that the pressure term has been eliminated, and the boundary conditions (11b) imply that the coupling of the problem is now on the boundary Γ.

3 Weakly imposed boundary conditions

As stated in the previous section, the main challenge is the numerical implementation of the boundary conditions (11b). In this section, we describe a variational approach to incorporate these boundary conditions based on the symmetric Nitsche method [12].

Let $\mathcal{T}_h$ be a shape regular finite element partitioning of the domain $\Omega \subset \mathbb{R}^2$. This partitioning naturally generates a set of edges $\mathcal{E}_h$ on the boundary Γ. Furthermore, the diameter of an edge $E \in \mathcal{E}_h$ is denoted by h_E.

We denote $H^1(\Omega)$ as the usual Sobolev space on Ω. The L^2-inner product is denoted by $(\cdot,\cdot)_\Omega$, where Ω is the domain of integration. We also define the function spaces

$$V_h = \left\{ \boldsymbol{v} \in H^1(\Omega)^2 : \boldsymbol{v}|_K \in \mathcal{P}_r(K)^2 \text{ for all } K \in \mathcal{T}_h \right\}$$

and

$$W_h = \left\{ w \in H^1(\Omega) : \int_\Omega w \, dx = 0 \text{ and } \boldsymbol{w}|_K \in \mathcal{P}_r(K) \text{ for all } K \in \mathcal{T}_h \right\},$$

where $\mathcal{P}_r(K)$ is the set of polynomials on an element $K \in \mathcal{T}_h$ with degree at most r. Using the symmetric Nitsche method to impose the boundary conditions (11b) leads to the following semi-discrete weak problem: find $(\boldsymbol{m}_h(t), \phi_h(t)) \in V_h \times W_h$ such that

$$\begin{aligned}
&(\partial_t \boldsymbol{m}_h(t), \boldsymbol{v}_h)_\Omega + \frac{1}{Re}(\nabla \boldsymbol{m}_h(t), \nabla \boldsymbol{v}_h)_\Omega - \frac{1}{Re}\sum_{E\in\mathcal{E}_h} (\nabla \boldsymbol{m}_h(t)\boldsymbol{n}, \boldsymbol{v}_h)_E \\
&- \frac{1}{Re}\sum_{E\in\mathcal{E}_h} (\boldsymbol{m}_h(t), \nabla \boldsymbol{v}_h \boldsymbol{n})_E + \frac{\gamma}{Re}\sum_{E\in\mathcal{E}_h} \frac{1}{h_E}(\boldsymbol{m}_h(t), \boldsymbol{v}_h)_E \\
&- \frac{1}{Re}\sum_{E\in\mathcal{E}_h} (P_\tau(\nabla \phi_h(t)), \nabla \boldsymbol{v}_h \boldsymbol{n})_E + \frac{\gamma}{Re}\sum_{E\in\mathcal{E}_h} \frac{1}{h_E}(P_\tau(\nabla \phi_h(t)), \boldsymbol{v}_h)_E \\
&= (\boldsymbol{f}(t), \boldsymbol{v}_h)_\Omega - (\nabla \boldsymbol{u}_h(t)\boldsymbol{u}_h(t), \boldsymbol{v}_h)_\Omega
\end{aligned} \tag{13}$$

and

$$(\nabla\phi_h(t), \nabla q_h)_\Omega = (\nabla \cdot \mathbf{m}_h(t), q_h)_\Omega \tag{14}$$

for all $(\boldsymbol{\nu}_h, q_h) \in V_h \times W_h$, where $\gamma > 0$ is the stabilization constant. Here, $P_{\boldsymbol{\tau}}(\boldsymbol{\nu}) = (I - \mathbf{n} \otimes \mathbf{n})\boldsymbol{\nu}$ is the tangential component of $\boldsymbol{\nu}$, where $\mathbf{n}$ and $\boldsymbol{\tau}$ denote the normal and tangential vectors, respectively.

Remark 3. We observe that the semi-discrete weak problem described above is a coupled problem, and hence the time discretization needs to be chosen such that the problem becomes computationally decoupled. This is discussed in more details in the next section.

Remark 4. The stabilization constant γ must be chosen large enough such that the coercivity of the problem is maintained, but not too large to avoid a significant loss in numerical accuracy [8]. Our choice of the stabilization constant is based on the common values chosen for the Poisson equation with Dirichlet boundary conditions [15, 11].

We now show that the weak problem (13)–(14) is consistent with the continuous problem (11)–(12).

Proposition 5. *The weak solutions of the problem* (11)–(12) *satisfy equations* (13)–(14).

Proof: Suppose that $(\mathbf{m}, \phi)$ is a weak solution of the problem (11)–(12). We first observe that $(\mathbf{m}, \phi)$ satisfies equation (14) since this equation is the standard weak formulation of the Poisson problem (12). Then, in order to show that the weak solution satisfies equation (13), we look at the boundary terms in this equation. Since the first boundary term emerged from integration by parts, it suffices to show that the other boundary terms vanish. To this end, we use the normal and tangential components of $\mathbf{m}$ and $\nabla\phi$ as follows:

$$P_{\boldsymbol{\tau}}(\nabla\phi) = (\nabla\phi \cdot \boldsymbol{\tau})\boldsymbol{\tau} \quad \text{and} \quad \mathbf{m} = (\mathbf{m}\cdot\mathbf{n})\mathbf{n} + (\mathbf{m}\cdot\boldsymbol{\tau})\boldsymbol{\tau} = (\mathbf{m}\cdot\boldsymbol{\tau})\boldsymbol{\tau} = -(\nabla\phi\cdot\boldsymbol{\tau})\boldsymbol{\tau}$$

for all $E \in \mathcal{E}_h$, where we have used the fact that $(\mathbf{m}, \phi)$ satisfies equation (11b). Therefore, we obtain

$$
\begin{aligned}
&-\frac{1}{\mathrm{Re}} \sum_{E \in \mathcal{E}_h} (\mathbf{m}, \nabla \boldsymbol{v}_h \mathbf{n})_E + \frac{\gamma}{\mathrm{Re}} \sum_{E \in \mathcal{E}_h} \frac{1}{h_E} (\mathbf{m}, \boldsymbol{v}_h)_E \\
&-\frac{1}{\mathrm{Re}} \sum_{E \in \mathcal{E}_h} (P_{\boldsymbol{\tau}}(\nabla \phi), \nabla \boldsymbol{v}_h \mathbf{n})_E + \frac{\gamma}{\mathrm{Re}} \sum_{E \in \mathcal{E}_h} \frac{1}{h_E} (P_{\boldsymbol{\tau}}(\nabla \phi), \boldsymbol{v}_h)_E \\
&= -\frac{1}{\mathrm{Re}} \sum_{E \in \mathcal{E}_h} (-(\nabla \phi \cdot \boldsymbol{\tau})\boldsymbol{\tau}, \nabla \boldsymbol{v}_h \mathbf{n})_E + \frac{\gamma}{\mathrm{Re}} \sum_{E \in \mathcal{E}_h} \frac{1}{h_E} (-(\nabla \phi \cdot \boldsymbol{\tau})\boldsymbol{\tau}, \boldsymbol{v}_h)_E \\
&-\frac{1}{\mathrm{Re}} \sum_{E \in \mathcal{E}_h} ((\nabla \phi \cdot \boldsymbol{\tau})\boldsymbol{\tau}, \nabla \boldsymbol{v}_h \mathbf{n})_E + \frac{\gamma}{\mathrm{Re}} \sum_{E \in \mathcal{E}_h} \frac{1}{h_E} ((\nabla \phi \cdot \boldsymbol{\tau})\boldsymbol{\tau}, \boldsymbol{v}_h)_E \\
&= 0,
\end{aligned}
$$

which concludes the proof. ♠

4 Time discretizations

In this section, we describe the time discretization of the semi-discrete weak problem (13)–(14). The main motivation is that the time discretization has to computationally decouple the problem and maintain accuracy. The time discretization presented here is based on the second-order backward differentiation formula, which is commonly used to numerically solve the Navier–Stokes equations [9].

Let us start with discretizing equation (13) using the second-order backward differentiation formula. Assuming a uniform time step $k > 0$, we denote the value of $\mathbf{m}_h$ at the nth time step as $\mathbf{m}_h^n$. It follows that we have

$$
\partial_t \mathbf{m}_h(t)|_{t=(n+1)k} \approx \frac{3\mathbf{m}_h^{n+1} - 4\mathbf{m}_h^n + \mathbf{m}_h^{n-1}}{2k},
$$

and the rest of the time-dependent terms $\nabla\phi_h$, $\mathbf{u}_h$, and $\mathbf{f}$ are replaced with $\nabla\phi_h^{n+1}$, $\mathbf{u}_h^{n+1}$ and $\mathbf{f}^{n+1}$, respectively. This leads to a fully discretized equation, and we need to extrapolate $\nabla\phi_h^{n+1}$ and $\mathbf{u}_h^{n+1}$ in order to computationally decouple the problem. For the gradient of the gauge variable $\nabla\phi_h^{n+1}$, we use the extrapolation

$$\nabla\phi_h^{n+1} \approx 2\nabla\phi_h^n - \nabla\phi_h^{n-1},$$

which is shown to be second-order accurate using normal mode analysis [18]. Applying a similar approach to the velocity $\mathbf{u}_h^{n+1}$ gives $\mathbf{u}_h^{n+1} \approx 2\mathbf{u}_h^n - \mathbf{u}_h^{n-1}$. Hence, using these extrapolations, it is now possible to solve for $\mathbf{m}_h^{n+1}$ given the value of all variables at the previous two time steps.

We now describe in detail the resulting algorithm. Initially, we compute $\mathbf{m}_h^1$, ϕ_h^1 and $\mathbf{u}_h^1$ using the projection method. Set a final time $T > 0$, and repeat for $n = 1, 2, \ldots, N$, where $N = \lfloor T/k - 1 \rfloor$.

1. Find $\mathbf{m}_h^{n+1} \in V_h$ such that

$$\begin{aligned}
&\left(\frac{3\mathbf{m}_h^{n+1} - 4\mathbf{m}_h^n + \mathbf{m}_h^{n-1}}{2k}, \boldsymbol{\nu}_h\right)_\Omega + \frac{1}{Re}(\nabla\mathbf{m}_h^{n+1}, \nabla\boldsymbol{\nu}_h)_\Omega \\
&- \frac{1}{Re}\sum_{E\in\mathcal{E}_h}(\nabla\mathbf{m}_h^{n+1}\mathbf{n}, \boldsymbol{\nu}_h)_E - \frac{1}{Re}\sum_{E\in\mathcal{E}_h}(\mathbf{m}_h^{n+1}, \nabla\boldsymbol{\nu}_h\mathbf{n})_E \\
&+ \frac{\gamma}{Re}\sum_{E\in\mathcal{E}_h}\frac{1}{h_E}(\mathbf{m}_h^{n+1}, \boldsymbol{\nu}_h)_E \\
&= (\mathbf{f}^{n+1}, \boldsymbol{\nu}_h)_\Omega - (\nabla(2\mathbf{u}_h^n - \mathbf{u}_h^{n-1})(2\mathbf{u}_h^n - \mathbf{u}_h^{n-1}), \boldsymbol{\nu}_h)_\Omega \\
&+ \frac{1}{Re}\sum_{E\in\mathcal{E}_h}(P_\tau(2\nabla\phi_h^n - \nabla\phi_h^{n-1}), \nabla\boldsymbol{\nu}_h\mathbf{n})_E \\
&- \frac{\gamma}{Re}\sum_{E\in\mathcal{E}_h}\frac{1}{h_E}(P_\tau(2\nabla\phi_h^n - \nabla\phi_h^{n-1}), \boldsymbol{\nu}_h)_E
\end{aligned}$$

for all $\boldsymbol{\nu}_h \in V_h$, where $P_\tau(\boldsymbol{\nu}) = (I - \mathbf{n}\otimes\mathbf{n})\boldsymbol{\nu}$.

2. Find $\phi^{n+1} \in W_h$ such that $(\nabla\phi^{n+1}, \nabla q_h)_\Omega = (\nabla \cdot \mathbf{m}_h^{n+1}, q_h)_\Omega$ for all $q_h \in W_h$.
3. Compute $\mathbf{u}_h^{n+1} = \mathbf{m}_h^{n+1} + \nabla\phi_h^{n+1}$.

Remark 6. We do not need to compute the pressure at each time step to carry out the algorithm. In the case where the pressure is a quantity of interest, we recover it by discretizing equation (6). For instance, in order to achieve a second-order accurate approximation, we utilize the Crank–Nicolson discretization

$$p_h^{n+1/2} = \frac{1}{2\,\mathrm{Re}}\Delta(\phi_h^{n+1} + \phi_h^n) - \frac{\phi_h^{n+1} - \phi_h^n}{k}.$$

5 Numerical results

In this section, we present some numerical results to demonstrate the accuracy of our proposed method. In particular, we perform numerical tests based on the method of manufactured solutions to verify that the proposed method is second-order accurate and does not produce inaccurate numerical boundary layers. The numerical computations for these tests are carried out using FEniCS [10].

Let us first briefly describe the numerical setup. We choose the 2D unit square $\Omega = [0,1]^2$ as the domain. The exact solutions are chosen as follows:

$$\begin{aligned} \mathbf{u}_e &= \begin{bmatrix} -\cos(t)\sin(\pi x)\sin(\pi x)\sin(2\pi y) \\ \cos(t)\sin(2\pi x)\sin(\pi y)\sin(\pi y) \end{bmatrix}, \\ \phi_e &= -\cos(t)\cos(\pi x)\cos(\pi y), \end{aligned} \tag{15}$$

and

$$p_e = (2\pi^2\cos t - \sin t)\cos(\pi x)\cos(\pi y). \tag{16}$$

Furthermore, we set the final time $T = 0.5$ and the stabilization constant $\gamma = 20$. Motivated by the Taylor–Hood element pair [7], we use P_2, P_2 and P_1

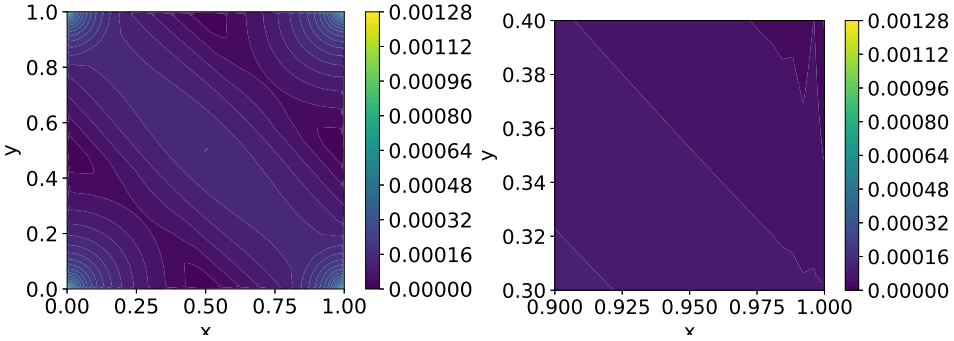

(a) Whole domain (b) Zoomed-in

Figure 2: Pressure error heatmaps obtained using the gauge method.

for $\mathbf{u}$, ϕ and p, respectively, where P_1 and P_2 denote the piecewise continuous linear and quadratic elements, respectively. The time step is chosen such that $k = O(h)$, where h is the spatial mesh size. We run the experiments for $h = 1/32, 1/64, 1/128, 1/256$. After that, we compute the rate of convergence $R_h = \log_2(\|e_h\|/\|e_{h/2}\|)$ using the L^1, L^2 and L^∞ norms, where $e_h = \mathbf{u}_e - \mathbf{u}_h$ for the velocity and $e_h = p_e - p_h$ for the pressure. Here $\mathbf{u}_h$ and p_h denote the numerical approximation of the velocity and pressure, respectively.

Figure 2 illustrates the pressure absolute value error heatmaps for $h = 1/256$. The left heatmap shows that the errors are focused at the corners of the domain, and the right heatmap verifies that there is no inaccurate numerical boundary layer. Furthermore, the convergence rates for both the velocity and pressure are illustrated in Tables 1–3 and Figures 3–4. It is inferred that both the velocity and pressure achieve the expected second-order accuracy.

Remark 7. From Figure 2, we observe that the errors at the corners are larger than the sides and interior of the domain. We argue that this is not a concern since it is demonstrated in Table 3 that the L^∞ norm of the error is second-order accurate.

Table 1: L^1 norm error, where $R_h = \log_2(\|e_h\|_{L^1}/\|e_{h/2}\|_{L^1})$.

h	$\mathbf{u}$		p	
	$\|e_h\|_{L^1}$	R_h	$\|e_h\|_{L^1}$	R_h
1/32	1.674E − 03	1.959	6.869E − 03	2.031
1/64	4.305E − 04	1.980	1.681E − 03	2.017
1/128	1.091E − 04	1.990	4.152E − 04	2.009
1/256	2.746E − 05		1.032E − 04	

Table 2: L^2 norm error, where $R_h = \log_2(\|e_h\|_{L^2}/\|e_{h/2}\|_{L^2})$.

h	$\mathbf{u}$		p	
	$\|e_h\|_{L^2}$	R_h	$\|e_h\|_{L^2}$	R_h
1/32	1.518E − 03	1.967	9.135E − 03	2.029
1/64	3.882E − 04	1.985	2.238E − 03	2.018
1/128	9.804E − 05	1.993	5.527E − 04	2.010
1/256	2.463E − 05		1.372E − 04	

Table 3: L^∞ norm error, where $R_h = \log_2(\|e_h\|_{L^\infty}/\|e_{h/2}\|_{L^\infty})$.

h	$\mathbf{u}$		p	
	$\|e_h\|_{L^\infty}$	R_h	$\|e_h\|_{L^\infty}$	R_h
1/32	4.101E − 03	1.990	6.414E − 02	1.868
1/64	1.032E − 03	1.998	1.757E − 02	1.884
1/128	2.585E − 04	2.000	4.759E − 03	1.894
1/256	6.461E − 05		1.281E − 03	

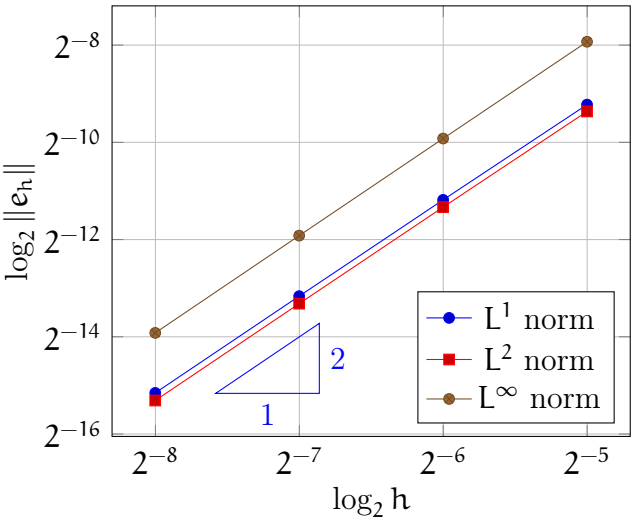

Figure 3: Convergence plot for $\mathbf{u}$.

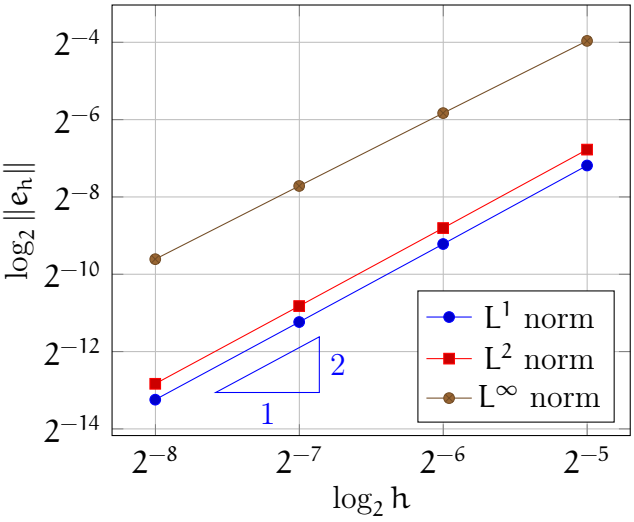

Figure 4: Convergence plot for $\mathfrak{p}$.

6 Conclusion

In this work, we have applied the symmetric Nitsche method to weakly impose the boundary conditions for the auxiliary vector field in the gauge formulation of the Navier–Stokes equations. Furthermore, we have described the appropriate time discretization for the resulting semi-discrete weak problem, and the detailed algorithm has been set out. Finally, we have verified via numerical experiments that our proposed method achieved the expected accuracy and did not suffer from inaccurate numerical boundary layers.

Acknowledgements The first author acknowledges financial support from an ANU University Research Scholarship.

References

[1] J. H. Bramble, J. E. Pasciak, and A. T. Vassilev. "Analysis of the Iinexact Uzawa algorithm for saddle point problems". In: *SIAM J. Numer. Anal.* 34.3 (1997), pp. 1072–1092. DOI: 10.1137/S0036142994273343 (cit. on p. C130).

[2] D. L. Brown, R. Cortez, and M. L. Minion. "Accurate projection methods for the incompressible Navier–Stokes equations". In: *J. Comput. Phys.* 168.2 (2001), pp. 464–499. DOI: 10.1006/jcph.2001.6715 (cit. on p. C131).

[3] A. J. Chorin. "The numerical solution of the Navier–Stokes equations for an incompressible fluid". In: *Bull. Amer. Math. Soc.* 73 (1967), pp. 928–931. DOI: 10.1090/s0002-9904-1967-11853-6 (cit. on p. C130).

[4] W. E and J.-G. Liu. "Gauge finite element method for incompressible flows". In: *Int. J. Numer. Meth. Fluids* 34 (2000), pp. 701–710. DOI: 10.1002/1097-0363(20001230)34:8<701::AID-FLD76>3.0.CO;2-B (cit. on pp. C131, C132).

[5] W. E and J.-G. Liu. "Projection method I: Convergence and numerical boundary layers". In: *SIAM J. Numer. Anal.* 32 (1995), pp. 1017–1057. DOI: 10.1137/0732047 (cit. on p. C130).

[6] W. Ef and J.-G. Liu. "Gauge method for viscous incompressible flows". In: *Commun. Math. Sci.* 1.2 (2003), pp. 317–332. DOI: 10.4310/CMS.2003.v1.n2.a6 (cit. on pp. C130, C131).

[7] A. Ern and J.-L. Guermond. *Theory and practice of finite elements*. Vol. 159. Applied mathematical sciences. Springer, 2004. DOI: 10.1007/978-1-4757-4355-5 (cit. on p. C138).

[8] P. Hansbo. "Nitsche's method for interface problems in computational mechanics". In: *GAMM-Mitteilungen* 28.2 (2005), pp. 183–206. DOI: 10.1002/gamm.201490018 (cit. on p. C135).

[9] W. Layton, N. Mays, M. Neda, and C. Trenchea. "Numerical analysis of modular regularization methods for the BDF2 time discretization of the Navier–Stokes equations". In: *Math. Model. Numer. Anal.* 48.3 (2014), pp. 765–793. DOI: 10.1051/m2an/2013120 (cit. on p. C136).

[10] A. Logg, K.-A. Mardal, and G. Wells. *Automated solution of differential equations by the finite element method: The FEniCS book*. Vol. 84. Lecture notes in computational science and engineering. Springer, 2012. DOI: 10.1007/978-3-642-23099-8 (cit. on pp. C131, C138).

[11] R. Mekhlouf, A. Baggag, and L. Remaki. "Assessment of Nitsche's method for Dirichlet boundary conditions treatment". In: *J. Fluid Flow, Heat Mass Trans.* 4.1 (2017), pp. 54–63. DOI: 10.11159/jffhmt.2017.007 (cit. on p. C135).

[12] J. Nitsche. "Über ein Variationsprinzip zur Lösung von Dirichlet-Problemen bei Verwendung von Teilräumen, die keinen Randbedingungen unterworfen sind". In: *Abh. Math. Semin. Univ. Hambg.* Vol. 36. Springer. 1971, pp. 9–15. DOI: 10.1007/BF02995904 (cit. on pp. C131, C134).

[13] R. H. Nochetto and J.-H. Pyo. "The gauge-Uzawa finite element method. Part I: The Navier–Stokes equations". In: *SIAM J. Numer. Anal.* 43.3 (2005), pp. 1043–1068. DOI: 10.1137/040609756 (cit. on pp. C131, C133).

[14] J.-H. Pyo. "Error estimates for the second order semi-discrete stabilized gauge-Uzawa method for the Navier–Stokes equations". In: *Int. J. Numer. Anal. Mod.* 10.1 (2013). URL: https://www.global-sci.org/intro/article_detail/ijnam/557.html (cit. on p. C131).

[15] L. Ridgway Scott. *Introduction to automated modeling with FEniCS*. Computational Modeling Initiative, 2018. URL: https://www.cminit.company/publications (cit. on p. C135).

[16] R. Temam. "Sur l'approximation de la solution des équations de Navier–Stokes par la méthode des pas fractionnaires (II)". In: *Arch. Rat. Mech. Anal.* 33.5 (1969), pp. 377–385. DOI: 10.1007/BF00247696 (cit. on p. C130).

[17] C. Wang and J.-G. Liu. "Convergence of gauge method for incompressible flow". In: *Math. Comput.* 69 (2000), pp. 1385–1407. DOI: 10.1090/S0025-5718-00-01248-5 (cit. on p. C131).

[18] K. Wiratama. "A comparison of projection and gauge methods for numerical incompressible fluid dynamics". Masters thesis. Australian National University, Oct. 2019 (cit. on pp. C130, C137).

[19] H. Zhang. "Application of projection methods to the numerical solution of the incompressible Navier Stokes equations". Honours thesis. Australian National University, Oct. 2014 (cit. on p. C131).

Author addresses

1. **Kenny Wiratama**, Mathematical Sciences Institute, Australian National University, Canberra, ACT 0200 AUSTRALIA
mailto:kenny.wiratama@anu.edu.au
orcid:0000-0003-0475-9180

2. **Stephen Roberts**, Mathematical Sciences Institute, Australian National University, Canberra, ACT 0200 AUSTRALIA
orcid:0000-0002-6730-3108

3. **Kenneth Duru**, Mathematical Sciences Institute, Australian National University, Canberra, ACT 0200 AUSTRALIA
orcid:0000-0002-5260-7942